SCIENCE CHINA
Technological Sciences

•Article•

November 2019 Vol.62 No.11: 2014–2020
https://doi.org/10.1007/s11431-019-9530-6

The influence mechanism of the strain rate on the tensile behavior of copper nanowire

ZHAO LeiYang & LIU Yan*

School of Aerospace Engineering, Tsinghua University, Beijing 100084, China

Received January 2, 2019; accepted May 24, 2019; published online October 14, 2019

The influence mechanism of the strain rate on the tensile behavior of the copper nanowires is investigated with molecular dynamics (MD) simulations. Three failure modes are observed at the loading strain rates from 5×10^{6} to 1×10^{9} s^{-1}. The three modes are named slipping mode, mixed mode and necking mode, respectively. The evolution of atomic configurations show that the competition of the lattice recovery and the dislocation multiplication determines the fracture mode, and the importance of lattice recovery decreases with the increase of strain rate. The input and the reflection of the tensile wave, which is induced by tensile loading, also plays an important role in the failure mechanism. The location of necking tends to approach the two ends of nanowire at higher strain rates.

strain rate effect, copper nanowire, molecular dynamics, dislocation, failure mode, lattice recovery

Citation: Zhao L Y, Liu Y. The influence mechanism of the strain rate on the tensile behavior of copper nanowire. Sci China Tech Sci, 2019, 62: 2014–2020, https://doi.org/10.1007/s11431-019-9530-6

1 Introduction

Novel materials at nanoscale possess many attractive properties [1–3]. In particular, metal nanowires receive considerable attention owing to their outstanding properties such as high strength [3–6], superplasticity [7,8] and electronic transport [9,10]. Obtaining credible values and exploring the underlying mechanisms of the aforementioned outstanding properties is of great interest in the research of nanowires.

Bending and nano-indentation experiments [11–13] were carried out to study the mechanical properties of nanowires. It was found that the Young's modulus of nanowire is independent of diameter while the yield strength increases as the decrease of diameter. The experimental investigations, though being widely focused on, are not easy to design and measure due to the tiny size of nanowires. Molecular dynamics (MD) simulation, as an alternative way, has been widely applied to study the mechanical behaviors of nanowires. Numerical results for the strength were consistent with the experimental observations, and it was observed that the strengthes of nanowires are much higher than the counterparts of bulk materials [3,5]. Various influential parameters, such as the temperature, the atomic structures, the loading orientations and the nanowire size have been investigated with MD. The variation of mechanical properties with the temperature was obtained [14–17]. Grain boundaries have significant effect on the yield strength and the ductility of the nanowires and bulk materials, which increase monotonically as the grain size decreases [18,19]. It was also observed that the Young's modulus and the yield strength of nanowires in orientations $<111>$ are larger than those in orientations $<100>$ [15,19,20]. MD simulations also come to the conclusion that the yield strength increases as the decrease of diameter [21–23].

However, the available time step size is limited at the order of femtosecond in MD simulations, which implies that the stain rates have to be orders higher than practical strain rates to make the computations feasible. Therefore the strain rate

*Corresponding author (email: yan-liu@tsinghua.edu.cn)

effect of nanowires must be investigated to connect the simulation results and the engineering applications. Efforts have been made to investigate mechanical properties under various strain rates, such as the superplasticity of nanowires at low strain rate and the amorphous state at high strain rate [7]. It was found that the yield stress of nanowire increases as the tensile loading rate increases [21,22]. When the nanowires are under compression, studies indicated that the buckling stress will remain constant after the strain rate reaches a critical value [24]. Some phenomena, such as slipping, necking and rearrangement of atomic configuration may disappear at very high strain rates [15]. However, the strain rate effect of nanowires is still not very clear due to high loading rates and small specimen sizes, and the underlying influence mechanism of strain rate has not been well revealed.

In this paper, we aim to investigate the mechanical behaviors of nanowires at relatively lower strain rates based on a series of MD simulations for the tensile process of copper nanowires. And we try to explore the failure modes and fracture mechanisms at various tensile strain rates.

2 Simulation methods

In this study, a cylindrical copper nanowire model of the length $210a_0$ and the diameter $20a_0$, as shown in Figure 1, was built, where a_0 is the lattice constant of copper. The coordinate axes of x, y, z are respectively along the crystal orientation [100], [010] and [001], and all directions are non-periodic boundary conditions.

The MD simulations were all performed using the LAMMPS package [25] with the time step of 1 fs, and the interatomic interactions were described using the embedded atom method (EAM) [26,27] potential. The computations were carried out on the Explorer 100 cluster system of Tsinghua University [28].

Nanowires were firstly relaxed at 300 K for 60 ps by using a Nosé-Hoover thermostat, then they were stretched with prescribed strain rates. Two rigid regions whose lengths are $5a_0$ are set at the two ends. The left region was defined as the fixed region, and the right was defined as the loading region. The atoms in the fixed region were fixed and those in the loading region were moved at a constant velocity corresponding to the loading rate. During the tension process, the atoms in the central region were kept at 300K in a canonical ensemble.

To investigate the influences of strain rate, 11 different loading strain rates in the range from 5×10^6 to 1×10^9 s^{-1} were applied in this work. These strain rates are comparable or smaller than those in previous works [29–32]. Central symmetry parameter (CSP) [33] and dislocation extraction algorithm (DXA) [34] were used to distinguish the evolution of atom structure during the tensile process, and images in this paper were created using OVITO package [35]. The stress σ_{xx} of all the Newtonian atoms in Figure 1 were computed to calculate the average stress of nanowire, and the atoms in the fixed region and loading region do not contribute.

3 Results and discussion

The stress-strain curves of nanowires at various strain rates ranging from 5×10^6 to 1×10^9 s^{-1} are shown in Figure 2(a) and (b). The elastic stages (AB) in all the curves are nearly identical, which implies that the Young's modulus is not influenced by the strain rate. However, the plastic deformation is influenced much by the strain rate. This is because the elastic property is determined by the harmonic vibration around the atomic equilibrium position. While the plastic deformation is determined by the dislocation nucleation, which should be strongly related with the strain rate.

The plastic part of the stress-strain curves for strain rates at 5×10^6–1×10^8 s^{-1} can be divided into three stages, including a sharp drop stage (BC), a hardening stage (CD) and a decrease with fluctuation stage (DE), as shown in Figure 2 (a). The curves in stage BC show two different modes: the yield stress almost does not change at 5×10^6–1×10^7 s^{-1} while the yield stress increases with the strain rate at 3×10^7 –1×10^8 s^{-1}. The tangential modulus of all curves in Figure 2 (a) are nearly the same in the hardening stage, which is also the same value as the initial linear stage. Similar to the first yield point, the strain at the second yield point does not change at 5×10^6–1×10^7 s^{-1} while it grows with the strain rate at 3×10^7–1×10^8 s^{-1}. In the stage DE, the stress in all curves reduce to zero gradually corresponding to the fact that the fracture of nanowires occurred before strain 0.3.

There are two stages in plastic deformation stage for strain rates 3×10^8–1×10^9 s^{-1}: a sharp drop stage (BC) and fluctuation stage (CD), as shown in Figure 2(b). It can be seen that the decline of stress is so large that the value of stress begin to fluctuate around zero, which indicate that nanowires have been broken. The existence of negative stress is caused by the springback of nanowire after breakage. The yield stress does not show obvious pattern about strain rates.

Figure 3 shows the three fracture modes corresponding to the above three types of stress-strain curves. The first fracture mode is the slipping mode at strain rates 5×10^6 –1×10^7 s^{-1}. The nanowire breaks along one slipping surface and the shape of the fracture surface is flat. The lattices in nanowire have enough time to recover at lower strain rate, and only few stacking faults occur at the breaking point. When the strain rate becomes very high (at 3×10^8–1×10^9 s^{-1}), the tensile process is too transient that local high stress cannot be released in such a short time span. The stacking

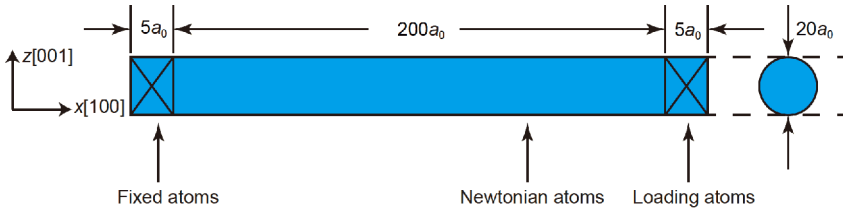

Figure 1 (Color online) Schematic view of the simulation model, which has fixed region and loading region at the ends.

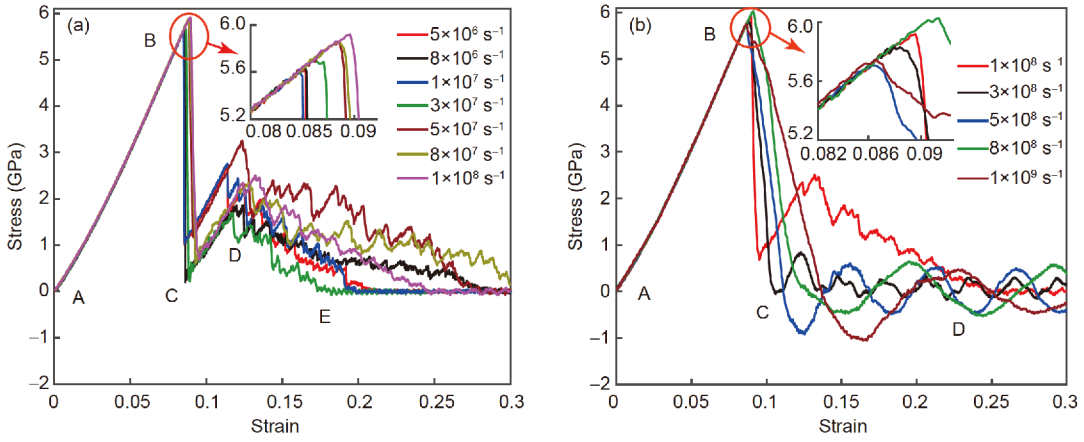

Figure 2 (Color online) Tensile stress-strain curves of copper nanowires at various strain rates. (a) Stress-strain curves at strain rates 5×10^6–1×10^8 s^{-1} with four stages: elastic stage (AB), sharp drop stage (BC), hardening stage (CD) and decreasing stage with fluctuation (DE); (b) stress-strain curves at strain rates 1×10^8–1×10^9 s^{-1} with three stages: elastic stage (AB), sharp drop stage (BC) and fluctuation stage (CD).

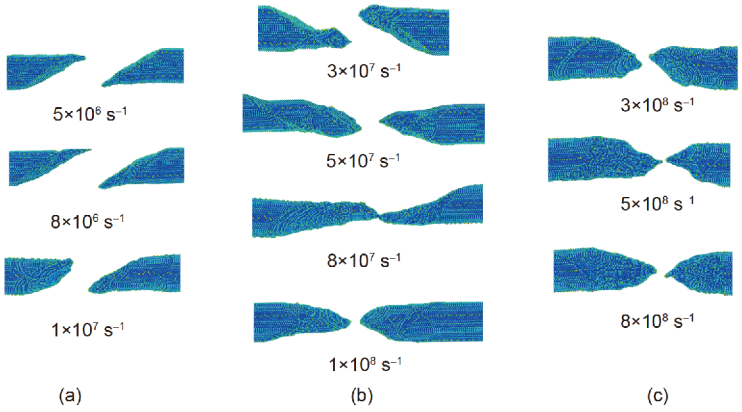

Figure 3 (Color online) Atomic configurations showing three fracture modes of copper nanowire at different strain rates. (a) Slipping mode. Nanowires break along one slipping surface and the fracture zone appears flat. (b) Mixed mode. Abundant stacking faults can be observed, and slipping trends and necking both exist. (c) Necking mode. Stacking faults are accumulated and necking is obvious.

faults are accumulated and breaking happens around the accumulation point. Different categories of stacking faults interact strongly, which is accompanied by obvious plastic necking deformation, as shown in Figure 3(c). Abundant stacking faults and necking can be both observed when the strain rate is between of 3×10^7–1×10^8 s^{-1}, which is named mixed mode. The slipping trend is obvious due to the stacking faults around the breaking point, however, the shape of the fracture surface is more like necking.

The dislocation analysis at different loading rates is shown in Figure 4. All the configuration snapshots are near the yield point and only atoms in HCP lattice are displayed, which shows the stacking faults in nanowires when the dislocation is just beginning to emit. Most dislocations are emitted from the surface of the nanowire, and stacking faults are induced after the emission of dislocations. The dislocation analysis also shows that almost all the dislocations are Shockley partial dislocation.

In order to further study the fracture mechanisms of different fracture mode, three representative cases,

5×10^6, 5×10^7 and 5×10^8 s^{-1} corresponding to slipping mode, mixed mode and necking mode respectively, are selected to show the evolution of atomic configurations. Each atom configuration includes the complete configuration and the local configuration of defects, where only internal atoms with a CSP value greater than 4 are displayed.

The evolution of atomic configuration at strain rate 5×10^6 s^{-1} is shown in Figure 5. The elastic stage of the stress-strain curve is omitted, and only the stress-strain curve of the plastic deformation stage is plotted in Figure 5. The first stacking fault appears at the yield point, then quick dislocation multiplication appears, as shown in Figure 5(a) and (b). However, the number of stacking faults decreases after the sharp drop of stress, which can be explained that the lattice recovery dominates over dislocation multiplication owing to stress relaxation. Multiple hardening after the yield point implies more dislocation activities, while enough lattice recovery inhibits the appearance of new stacking fault due to the low strain rate. The nanowire breaks between the stacking faults which are on the same slipping system, as shown in Figure 5(d) and (e).

Nanowires are loaded by moving right loading regions at a constant velocity corresponding to the strain rate, which is close to the common tensile experiment at macroscopic scale. Because the tensile velocity is in orders beyond the macroscopic quasi-static tensile velocity, the wave propagation is a significant factor in the failure of nanowires. Three regions of the length $5a_0$ as shown in Figure 6(a), are selected to monitor the local stress of nanowires to capture stress variation, and then to investigate the influence of wave propagation. The amplitude of stress wave is doubled when the stress wave propagates to and is reflected by the fixed end, whose effect can be observed from stress curves of left region and right region in Figure 6(b). The doubled stress amplitude make the local stress obviously exceed yield stress at higher strain rates, which causes that the damage is always near the end of nanowires. Furthermore, the physical time that the stress wave approaches to the fixed end determines the yield strain, hence the yield points seem irregular in Figure 2(b).

The evolution of atomic configurations at strain rate 5×10^8 s^{-1} is shown in Figure 7, and the stress-strain curves of the entire domain and three subdomains are also given. Abundant dislocations are emitted simultaneously at fixed

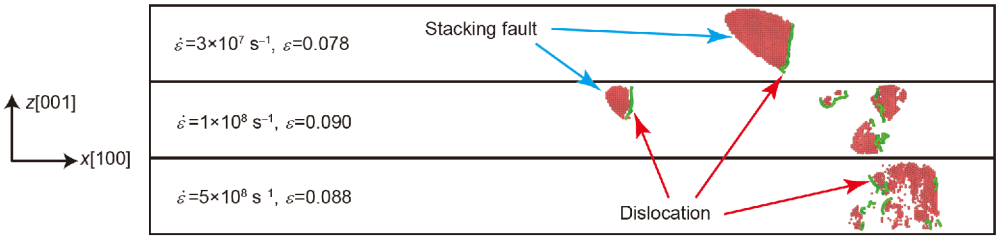

Figure 4 (Color online) The dislocation analysis of copper nanowires at different loading rates, and only atoms in HCP lattice and dislocations are displayed.

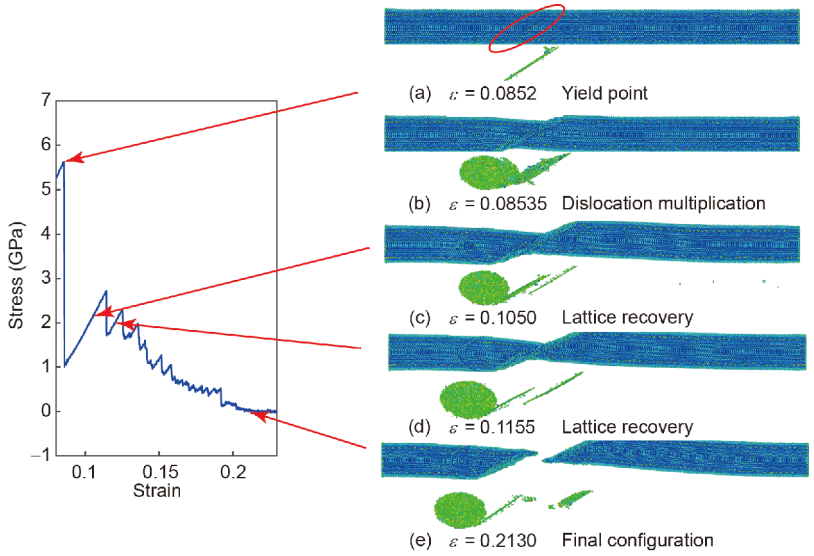

Figure 5 (Color online) Tensile process of copper nanowire at a constant loading rate of 5×10^6 s^{-1}. The left subgraph is the stress-strain curve while the right subgraphs are snapshots of atomic configuration at various tensile strains, as indicated by arrows.

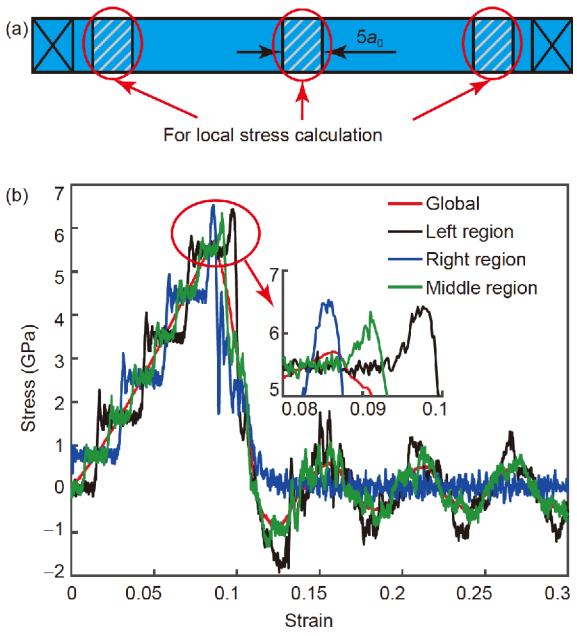

Figure 6 (Color online) The variation of stress in different domains at strain rate of 5×10^8 s^{-1}. (a) Schematic diagram of the subdomains for the calculation of the local stress. The three subdomains are marked as left region, middle region and right region in the stress-strain figure. (b) Stress-strain curve of the entire domain and three subdomains of nanowires.

end due to the excessive local stress, which causes stacking faults interact strongly and necking appears. Stress is not sufficiently released in stage BC due to the high strain rate, therefore the dislocation multiplication is at dominant position over lattice recovery, which is shown in Figure 7(b) and (c). The fracture happens quickly after the stress drop, and the lattice recovery appears after the fracture owing to lower stress level. Apparent stress fluctuation also leads to new stacking faults, consequently the competition of dislocation multiplication and lattice recovery results in the final configuration of nanowire in Figure 7(e).

It can be predicted that the two competition mechanisms are comparable at middle strain rates, as shown in Figure 8. The stacking faults exist at several locations in the nanowire at the yield point due to inadequate release of stress. However, the sharp drop of stress makes it possible that lattice recovery reduces stacking faults. Multiple slippage of nanowires makes the hardening stage more obvious, and weaker lattice recovery cannot inhibit stronger dislocation multiplication, which causes the stacking faults appear in several locations. Both lattice recovery and dislocation multiplication are important in Figure 8(c) and (d). The necking phenomena are found at several locations in addition to the fracture, but the necking development is different at different locations.

The fracture modes and mechanisms at different strain rates may also be affected by the length of nanowires, therefore a preliminary study of another two lengths ($110a_0$ and $310a_0$) was carried out based on the above work. The stress-strain curves of nanowires with different sizes are shown in Figure 9. The tensile stiffness of stress-strain curves has a slight variation, which should be related to the surface energy of nanowires. The local stress, which comes from the loading velocity, is dependent on the length of nanowire. A shorter nanowire will cause the mixed mode to appear at higher strain rates due to the decrease of local stress. The stress-strain curves of different lengths share common features. And the features can be well explained based on aforementioned discussions, which suggests that the fracture modes and mechanisms can be extended to nanowires of different sizes. More about the nanowires of

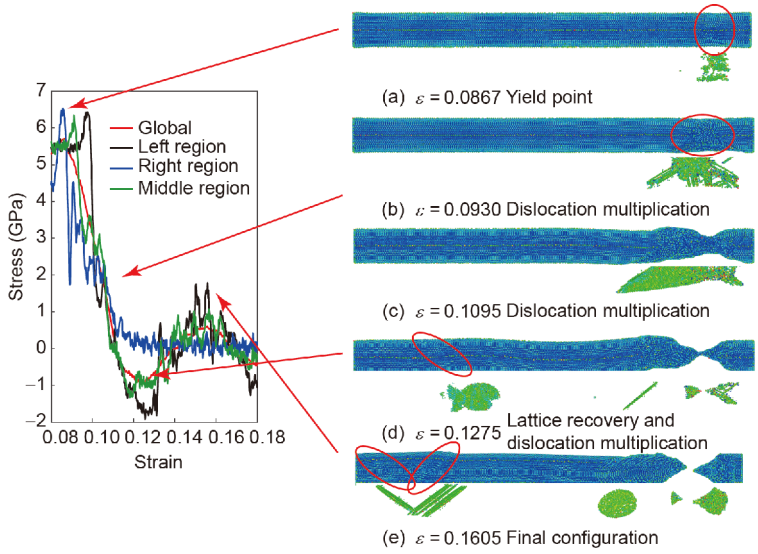

Figure 7 (Color online) Tensile process of copper nanowire at a constant loading rate 5×10^8 s^{-1}. The left subgraph is the stress-strain curve while the right subgraphs are snapshots of atomic configuration at various tensile strains, as indicated by arrows.

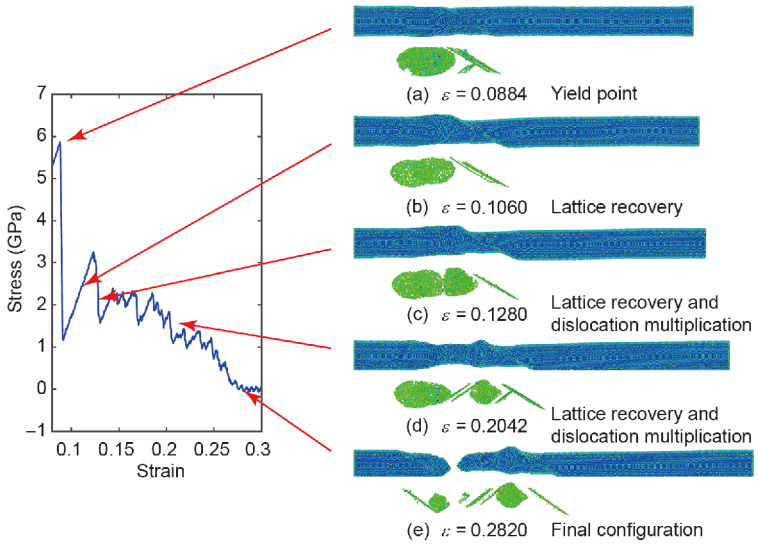

Figure 8 (Color online) Tensile process of copper nanowire at a constant loading rate 5×10^{7} s^{-1}. The left subgraph is the stress-strain curve while the right subgraphs are snapshots of atomic configuration at various tensile strains, as indicated by arrows.

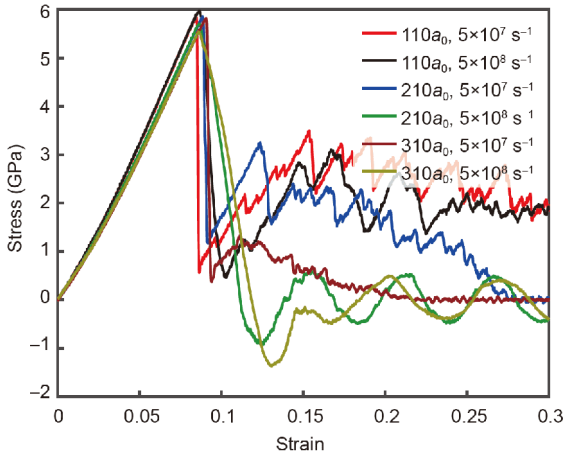

Figure 9 (Color online) Tensile stress-strain curves of copper nanowires of different sizes at strain rates 5×10^{7} and 5×10^{8} s^{-1}.

different sizes will be investigated in future research.

4 Conclusions

The influences of strain rates on the failure modes and failure mechanism of the copper nanowire are investigated in this paper with the molecular dynamics, and the loading rate is 5×10^{6}–1×10^{9} s^{-1}. The stress-strain curves and the evolution of configurations and defects at various strain rates are given. It is found that the strain rates can be classified into three categories. The yield stress does not vary for lower strain rates, increases with the strain rate at middle strain rates, but may decrease at much higher strain rates. The slipping mode, the mixed mode and the necking mode are observed for the lower rates, the middle rates and the higher rates respectively. The reason for the formation of the three modes are throughly discussed. The failure mechanism of the nanowires is the competition of the lattice recovery and the dislocation multiplication.

Future research may include the influence of the loading directions and the initial defects. Multiscale computation will be introduced to enlarge the available temporal and spatial scales.

This work was supported by the National Natural Science Foundation of China (Grant Nos. 11772171, 11672154), and the Science Challenge Project (Grant No. TZ2018001).

1 Bachtold A, Hadley P, Nakanishi T, et al. Logic circuits with carbon nanotube transistors. Science, 2001, 294: 1317–1320
2 Wang B, Zhang H B, Huang L J, et al. Evolution of microstructure and high temperature tensile properties of as-extruded TiBw reinforced near-α titanium matrix composite subjected to heat treatments. Sci China Tech Sci, 2018, 61: 1340–1345
3 Gall K, Diao J, Dunn M L. The strength of gold nanowires. Nano Lett, 2004, 4: 2431–2436
4 Philippe L, Peyrot I, Michler J, et al. Yield stress of monocrystalline rhenium nanowires. Appl Phys Lett, 2007, 91: 111919
5 Lao J, Naghdi Tam M, Pinisetty D, et al. Molecular dynamics simulation of fcc metallic nanowires: A review. J Miner Metal Mater Soc, 2013, 65: 175–184
6 Zheng Y G, Zhao Y T, Ye H F, et al. Size-dependent elastic moduli and vibrational properties of fivefold twinned copper nanowires. Nanotechnology, 2014, 25: 315701
7 Branício P S, Rino J P. Large deformation and amorphization of Ni nanowires under uniaxial strain: A molecular dynamics study. Phys Rev B, 2000, 62: 16950–16955
8 Wang B, Shi D, Jia J, et al. Elastic and plastic deformations of nickel nanowires under uniaxial compression. Phys E-Low-Dimensional Syst Nanostruct, 2005, 30: 45–50
9 Qin M, Shang Y, Wang X, et al. Mg doping and native N vacancy effect on electronic and transport properties of AlN nanowires. Sci China Tech Sci, 2015, 58: 832–839

10 Wang L F, Xu Z, Yang S Z, et al. Real-time *in situ* TEM studying the fading mechanism of tin dioxide nanowire electrodes in lithium ion batteries. Sci China Tech Sci, 2013, 56: 2630–2635
11 Li X, Gao H, Murphy C J, et al. Nanoindentation of silver nanowires. Nano Lett, 2003, 3: 1495–1498
12 Wu B, Heidelberg A, Boland J J. Mechanical properties of ultrahigh-strength gold nanowires. Nat Mater, 2005, 4: 525–529
13 Ni H, Li X, Gao H. Elastic modulus of amorphous SiO_2 nanowires. Appl Phys Lett, 2006, 88: 043108
14 Wu H A. Molecular dynamics study of the mechanics of metal nanowires at finite temperature. Eur J Mech-A/Solids, 2006, 25: 370–377
15 Chen D L, Chen T C. Mechanical properties of au nanowires under uniaxial tension with high strain-rate by molecular dynamics. Nanotechnology, 2005, 16: 2972–2981
16 Sainath G, Choudhary B K. Atomistic simulations on ductile-brittle transition in 111 BCC Fe nanowires. J Appl Phys, 2017, 122: 095101
17 Sun H L, Chen L Y, Sun S, et al. Size- and temperature-dependent Young's modulus and size-dependent thermal expansion coefficient of nanowires. Sci China Tech Sci, 2018, 61: 687–698
18 Zheng Y, Lu J, Zhang H, et al. Strengthening and toughening by interface-mediated slip transfer reaction in nanotwinned copper. Scripta Mater, 2009, 60: 508–511
19 Zhu W, Wang H, Yang W. Orientation- and microstructure-dependent deformation in metal nanowires under bending. Acta Mater, 2012, 60: 7112–7122
20 Wu H A. Molecular dynamics study on mechanics of metal nanowire. Mech Res Commun, 2006, 33: 9–16
21 Liang W, Zhou M. Response of copper nanowires in dynamic tensile deformation. Proc Institution Mech Engineers Part C-J Mech Eng Sci, 2004, 218: 599–606
22 Yuan F, Huang L. Molecular dynamics simulation of amorphous silica under uniaxial tension: From bulk to nanowire. J Non-Crystalline Solids, 2012, 358: 3481–3487
23 Sainath G, Choudhary B K, Jayakumar T. Molecular dynamics simulation studies on the size dependent tensile deformation and fracture behaviour of body centred cubic iron nanowires. Comput Mater Sci, 2015, 104: 76–83
24 Tang C Y, Zhang L C, Mylvaganam K. Rate dependent deformation of a silicon nanowire under uniaxial compression: Yielding, buckling and constitutive description. Comput Mater Sci, 2012, 51: 117–121
25 Plimpton S. Fast parallel algorithms for short-range molecular dynamics. J Comput Phys, 1995, 117: 1–19
26 Daw M S, Baskes M I. Embedded-atom method: Derivation and application to impurities, surfaces, and other defects in metals. Phys Rev B, 1984, 29: 6443–6453
27 Foiles S M, Baskes M I, Daw M S. Embedded-atom-method functions for the fcc metals Cu, Ag, Au, Ni, Pd, Pt, and their alloys. Phys Rev B, 1986, 33: 7983–7991
28 Zhang W, Lin J, Xu W, et al. Scstore: Managing scientific computing packages for hybrid system with containers. Tsinghua Sci Technol, 2017, 22: 675–681
29 Li L, Han M. Molecular dynamics simulations on tensile behaviors of single-crystal bcc Fe nanowire: Effects of strain rates and thermal environment. Appl Phys A, 2017, 123: 450
30 Zhang X, Li X, Gao H. Size and strain rate effects in tensile strength of penta-twinned Ag nanowires. Acta Mech Sin, 2017, 33: 792–800
31 Chang L, Zhou C Y, Wen L L, et al. Molecular dynamics study of strain rate effects on tensile behavior of single crystal titanium nanowire. Comput Mater Sci, 2017, 128: 348–358
32 Xie H, Yin F, Yu T, et al. A new strain-rate-induced deformation mechanism of Cu nanowire: Transition from dislocation nucleation to phase transformation. Acta Mater, 2015, 85: 191–198
33 Kelchner C L, Plimpton S J, Hamilton J C. Dislocation nucleation and defect structure during surface indentation. Phys Rev B, 1998, 58: 11085–11088
34 Stukowski A, Bulatov V V, Arsenlis A. Automated identification and indexing of dislocations in crystal interfaces. Model Simul Mater Sci Eng, 2012, 20: 085007
35 Stukowski A. Visualization and analysis of atomistic simulation data with OVITO-the open visualization tool. Model Simul Mater Sci Eng, 2009, 18: 015012